Lattice dynamics of the potential-induced breathing model: Phonon dispersion in the alkaline-earth oxides

Ronald E. Cohen, L. L. Boyer, and M. J. Mehl
Naval Research Laboratory, Washington, D.C. 20375-5000
(Received 4 August 1986)

We find the dynamical matrix for the potential-induced breathing (PIB) model for ionic solids, and calculate with no adjustable parameters the phonon-dispersion relations for the alkaline-earth oxides in the $B1$ structure. Our approach is similar to that of Gordon and Kim, in which the crystalline charge densities are estimated by overlapping atomic charge densities, which are then converted to energy by electron-gas approximations. It goes beyond the original Gordon-Kim model by allowing for spherical breathing of the atoms in response to the long-range potential, and beyond later refinements of the modified-electron-gas models by *explicitly* including the effects of PIB on the self-energy and the overlap interactions. This allows us to treat general deformations and lattice dynamics including the many-body PIB effects. PIB couples the long- and short-range forces in a way that is not present in any other lattice-dynamical model, since the spherical charge relaxation is coupled to the long-range electrostatic potential. PIB gives better agreement for the splitting of the longitudinal- and transverse-optic mode frequencies than is found with rigid-ion models, as well as much improved acoustic branches. PIB is a nonempirical model; no experimental data are used other than the values of fundamental constants such as Planck's constant and the atomic masses.

I. INTRODUCTION

In Gordon-Kim models,[1] the internal energy for a system is calculated from the energy of overlapping atomic charge densities using a local-density or electron-gas formalism. Gordon-Kim calculations are fast and inexpensive, compared to elaborate electronic structure methods, and give good estimates of physical properties of ionic solids without resort to experimental data.[2] To apply this model to oxides, the O^{2-} ion must be stabilized since O^{2-} is not stable in the free state. This is usually done with a Watson sphere of positive charge.[3] Paschalis and Weiss[3(b)] suggested that the Watson-sphere radius should be chosen to give the Madelung potential at the site in the crystal, and this procedure is now followed in most applications of the Watson-sphere model to ionic crystals. The model assumes that O^{2-} is stabilized in the crystal by the long-range electrostatic potential at the oxygen site, which leads to breathing of the charge density in response to the Madelung site potential. We call this effect potential-induced breathing (PIB). The coupling between the charge density and the long-range potential should be present regardless of the stability of the free ion, so we include Watson spheres and consider PIB for all cations and anions. The inclusion of Watson spheres in atomic calculations should provide charge densities which better model ions in crystals, in contrast to free atoms.

The PIB model differs from the requirement of self-consistency between the Watson-sphere potential and the electrostatic potential introduced in Ref. 2(b). In PIB the total-energy expression explicitly includes the self-energy and the coupling between the long-range and short-range forces. The site-matching technique, on the other hand, is a rigid-ion-type model for a charge density consistent with the electrostatic potential. Later improvements of the modified-electron-gas (MEG) model[2(e),2(f)] include the self-energy contribution to the pressure *ex post facto*.

PIB affects the calculated static and dynamic properties of solids,[4,5] and a marked improvement was found over rigid-ion models for static equations of state and elastic constants of the alkaline-earth oxides.[5] The effective many-body forces in PIB lead to the observed violations of the Cauchy equality (e.g., $C_{44}=C_{12}$). In contrast, rigid-ion models with central forces cannot violate the Cauchy equality, and breathing-shell models do not give the correct signs for the deviations.[6] The PIB model also decreases the predicted LO-TO splitting, giving values closer to experiment.[4] In Ref. 4 only some of the PIB contributions to the dynamical matrix were considered; the complete PIB dynamical matrix is derived here. The dispersion relations for the alkaline-earth oxides are calculated and compared with experiment.

With the PIB model, we can rapidly calculate static and vibrational properties of crystalline ionic solids, including thermal equations of state, elasticity, instabilities, and phase transitions. In general, elaborate methods for calculating electronic structure and total energy cannot yet be used to calculate static properties for complex crystals or lattice-dynamical properties of even simple solids for arbitrary wave vectors. Thus to calculate thermal properties, simple models such as the PIB model are necessary. While many empirical models are available,[6-8] they are generally limited to the interpretation of existing experimental results. On the other hand, nonempirical models such as the PIB model do not contain adjusted parameters and are therefore more powerful.

Simple nonempirical methods have been successful in calculating thermal equations of state and instabilities. For example, much progress has been made in understanding alkali halides and halide-based perovskites,[9]

melting, melt structure,[10] and ferroelectricity.[9(d)]

In Sec. II we discuss the PIB model, in Sec. III the calculational methods are shown, and in Sec. IV we give the results for the alkaline-earth oxides MgO, CaO, SrO, and BaO in the $B1$ structure. The results are discussed and compared with other models and experiments in Sec. V. The laborious parts of the derivation of the dynamical matrix are given in the Appendixes: In Appendix A, we derive the dynamical matrix elements, in Appendix B, an Ewald-type transformation for a lattice sum that arises in A is derived, and in Appendix C the equation used for the shift in the local potential is given.

II. THE PIB MODEL

A. Gordon-Kim models

Gordon and Kim[1] developed a powerful and simple method for calculating properties of closed-shell systems. The charge density is estimated by overlapping atomic charge densities. This procedure has shown considerable success since the ground-state properties of a system are completely specified by its charge density.[11] In a Gordon-Kim model, the energy is a sum of three parts: the electrostatic Madelung energy between the ions, the overlap energy between ions, and the self-energy of each ion. The importance of the latter contribution was neglected for some time, but inclusion of this term is necessary when a Watson sphere is included in the atomic calculation.

B. The Watson-sphere model

Some ions are not stable in the free state but are present in crystals. Watson[3(a)] introduced the idea of stabilizing O^{2-} by including a sphere of charge in the atomic calculation. (He attributed the idea of Slater.) The sphere corrects for the Coulomb repulsion of an electron at long distances from the atom. The Watson sphere commonly used in Gordon-Kim models is a sphere with charge equal and opposite to that of the ion, and a radius chosen to equal the Madelung site potential at the oxygen site in the crystal.[3(b),3(c)] The primary justification for the model has been its ability to produce excellent agreement with experiment, in contrast with other oxygen charge densities.[3(c)] The potential induced breathing implied by the Watson sphere model is a zeroth-order form of charge relaxation that has been left out of other lattice-dynamical models, such as shell models.

The physics behind the stabilization of O^{2-} in a crystal involves more than an electrostatic effect. It must to some extent also depend on the type of neighbors, for example Mg^{2+} in MgO or Ca^{2+} in CaO. Nevertheless the Madelung potential does play an important part in the stabilization. Consider an F center, an oxygen vacancy containing two electrons, in an oxide. An F center represents a probe, in a sense, that measures the environment that an oxygen ion sees in a crystal. Recent band-structure calculations for MgO and CaO using a muffin-tin Green's-function approach show that the F-center charge density is approximately an s state centered around the vacancy.[12] Elaborate calculations for an F center as a function of cell parameter have not yet been done, but as the potential well deepens at an F center relative to the surroundings of the vacancy the electrons are most probably more strongly localized. The F center charge density will breathe in response to the electrostatic potential.

Each oxygen in a crystal responds to the potential from the rest of the crystal. The same electrostatic forces that stabilize an F center stabilize an O^{2-} in the crystal, and the oxygen charge density will vary with changes in the electrostatic potential *relative to its surroundings.*

By equating the Watson sphere potential to the Madelung potential we are implicitly assuming that the short-range interactions involved in the stabilization of oxygen are essentially constant, and therefore can be ignored in the dynamical treatment. One could equate the Watson-sphere potential to the Madelung potential plus some constant that is optimized to give the best charge density relative to an electronic structure calculation; we intend to study this in the future. On the other hand, experience has shown that quite reasonable results are obtained without this added complication.

C. The dynamical matrix

The total potential energy in the PIB model is given by[4,5]

$$\Phi=\frac{1}{2}\sum_{\substack{l,l'\\k,k'}}{}'\frac{z_k z_{k'}}{|\mathbf{r}(^l_k)-\mathbf{r}(^{l'}_{k'})|}+\sum_{l,k}S_k(P(^l_k))$$
$$+\frac{1}{2}\sum_{\substack{l,l'\\k,k'}}{}'\phi_{kk'}(P(^l_k),P(^{l'}_{k'}),|\mathbf{r}(^l_k)-\mathbf{r}(^{l'}_{k'})|)\,, \qquad (1)$$

where the first term is the Madelung energy, the second term is the self-energy, and the third term is the overlap, or short-range, energy. The overlap energy is a function of the nuclear separation, and the overlap and self-energies are functions of the Madelung site potential, $P(^l_k)$. The indices l represent triplets of numbers indexing each primitive cell, and the indices k label each crystallographic site, or basis vector. A prime in a sum means that the interaction of an atom with itself is omitted.

The dynamical matrix is found by expanding the potential energy in a Taylor series to second order in displacements around the equilibrium atomic positions. An atomic displacement changes the site potentials at all the other atoms in the crystal.

The dynamical matrix contribution from the derivatives of the Madelung energy give the Coulomb contributions to the dynamical matrix found by Kellerman.[13,14] These contribution are irregular at $q=0$ due to the term proportional to $q_\alpha q_\beta/q^2$, which leads to a splitting of the LO and TO modes at any small but finite wave vector $\mathbf{q}$.

The derivatives of the dynamical matrix elements for the overlap and self-energy terms are given in Appendix A. In addition to the rigid-ion contributions,[15] we find terms that consist of sums of products of first derivatives of the Madelung potential and second derivatives of the short-range potentials and self-energies, and terms that consist of sums of products of second derivatives of the Madelung potential and first derivatives of the short-

range potentials and self-energies. The latter contributions to the dynamical matrix result in effective charges in the Kellerman coefficients, which are lower in magnitude than the ionic valences. They lead to a smaller LO-TO splitting than is obtained in a rigid-ion model.[4]

The terms containing first derivatives of the Madelung potential contain sums of the form (B1). This is the first derivative of the Madelung potential at sublattice j with respect to the amplitude of a displacement wave on sublattice k. This sum, referred to here as the Θ sum, is only slowly convergent. Appendix B gives a transformation into two rapidly convergent sums in direct space, and reciprocal space, respectively.

The PIB model considers absolute changes in the local electrostatic potential, rather than relative changes. If one does not correct for shifts in the local electrostatic zero, the LO branch diverges at long wavelengths since the theta sum diverges as $1/q$ as $q \rightarrow 0$. Furthermore, in structures more complex than rocksalt, translational invariance is not satisfied as the acoustic modes do not go to zero frequency as $q \rightarrow 0$. The solutions to these problems are discussed next.

D. The polarization shift

The atomic charge density should respond to changes in the local electrostatic potential, but it should not breathe in response to a uniform change in the local potential. The necessity to consider the relative potential causes no problem in static energy calculations. The Ewald technique fixes the average potential of the crystal and thus defines an electrostatic zero to which the site potentials are referred.[16] If the crystal structure is deformed by a longitudinal modulation, however, the local zero for the electrostatic potential becomes poorly defined. A modulation of the potential is superimposed on the rapid local potential variations and an unambiguous local zero cannot be defined for a longitudinal-optical phonon. However, as we shall see, an average local zero can be defined to a good approximation.

At long wavelengths this problem is related to the problem in defining an electrostatic zero in the first place. In Ewald's method, the average crystal potential is defined to be zero by effectively including a compensating uniform background charge density.[16] If the average potential were not fixed in this way, the Madelung potentials for each sublattice would be infinite. For long wavelengths, in fact, a nondivergent LO branch, and elastic constants identical to those obtained by static deformations are recovered if a uniform background is included in the Θ sum. In static calculations, the uniform backgrounds cancel because of charge neutrality of the crystal, whereas in the Θ sum they do not.

We are not only interested in the long-wavelength limit, but in arbitrary wave vectors. Since the polarization sets up the potential wave, we find a local average polarization and derive the potential shift caused by that average polarization. A Gaussian average has useful properties we can exploit, so a Gaussian average of the polarization is found and the corresponding derivative of the potential shift is subtracted from the Θ sum (Appendix C). With this correction for the local-potential zero, the elastic constants derived from the lattice dynamics and from static deformations agree with each other, and the LO branch no longer diverges at $q=0$.

III. METHODS

The atomic charge densities can be obtained by any method, and are typically obtained by Hatree-Fock calculations or density-functional methods. We obtain charge densities using density-functional theory[17] with the Liberman program.[18] The atomic charge densities are calculated fully relativistically using an effective potential including the Hedin-Lundqvist parametrization of the local exchange-correlation potential,[19] and averaged self-interaction corrections.[20] A Watson sphere of charge opposite to that of the ion is included in the calculation, and charge densities are calculated for different sphere radii.

The short-range, overlap contributions to the interatomic potentials are separated into five contributions. The short-range corrections to the Madelung energy are separated into electron-electron and electron-nuclear parts. These contributions correct for the finite size of the ions so that the electrostatic energy is calculated exactly for the model crystal charge density. The kinetic, exchange, and correlation energies are approximated as local functionals of the charge density. The Thomas-Femi kinetic energy functional ($\rho^{5/3}$) is used,[21] along with the Hedin-Lundqvist exchange and correlation. The use of the Thomas-Fermi functional is probably the largest error in our potentials, and corrections to this approximation are being studied. This simple approximation appears to provide good estimates for all structures and properties investigated so far.

We obtain nonempirical pair potentials in numerical form for pairs of atoms as functions of nuclear separation and Watson-sphere radii. The dynamical matrix elements could be obtained directly from the numerical potentials, but we find it convenient to express the numerical results in terms of analytic functions. These analytic functions reproduce the calculated potentials accurately.[5(b)]

The self-energy is calculated using the same functionals as for the overlap contributions, i.e., the Thomas-Fermi kinetic energy and the Hedin-Lundqvist exchange-correlation potential. Since the PIB effect causes charge to move in and out of the overlap region, it is important to use the same functionals for the atom and for the overlap. The use of different functionals would introduce a systematic error.

The electrostatic Madelung energy and the site potentials are calculated using the method of Ewald.[16] The potentials for the Watson spheres are taken as the Madelung potential at the nucleus. Local corrections to the electrostatic potential are not included since they would introduce a self-consistency requirement, and it would not then be possible to directly obtain the overlap potentials simply in terms of site potentials and nuclear separation.

Ref. 5(b) discusses the method in more detail. The only difference in the potentials used here and in Ref. 5 is the electron-nuclear part of the local correction to the electrostatic energy. In Ref. 5(b) a different analytic function was used for each atom for this contribution to the poten-

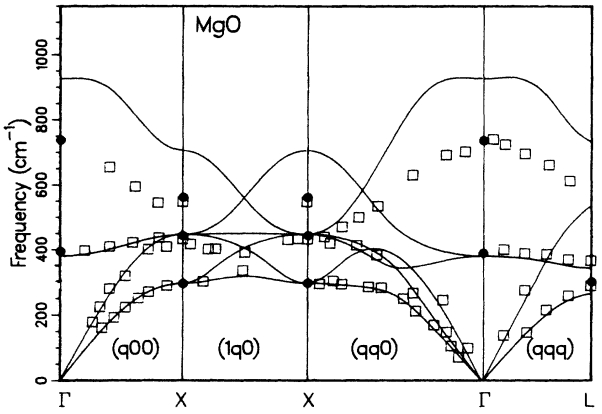

FIG. 1. Phonon dispersion relations for MgO. The solid lines are calculated with the PIB model using no adjustable parameters. The squares are from neutron scattering data [Refs. 7 and 22(a)] and the solid circles are derived from an interpretation of second-order Raman data [Ref. 23(a)].

tial. Here we use a single analytic function for each atom pair for this part, and thus treat the electron-nuclear and electron-electron parts of the local electrostatic correction in the same way.

IV. RESULTS AND DISCUSSION

A. Dispersion curves

Calculated dispersion curves for the alkaline earth oxides in the $B1$ structure are shown in Figs. 1—4. Neutron scattering[8,22] and second-order Raman data[23] are shown for comparison. (The second-order Raman data are based on neutron scattering data and/or comparisons among the alkaline-earth oxides for peak assignments. Since the spectra contain contributions from the entire Brillouin zone, the normal-mode frequencies derived from the spectra have relatively poor precision compared with neutron scattering data. Nevertheless, agreement between the Raman and neutron data are generally good.)

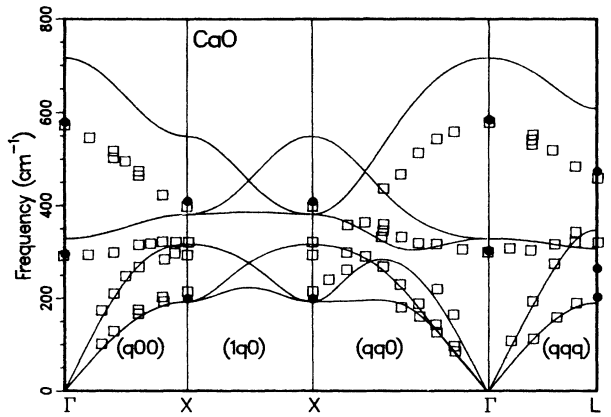

FIG. 2. Phonon dispersion relations for CaO.

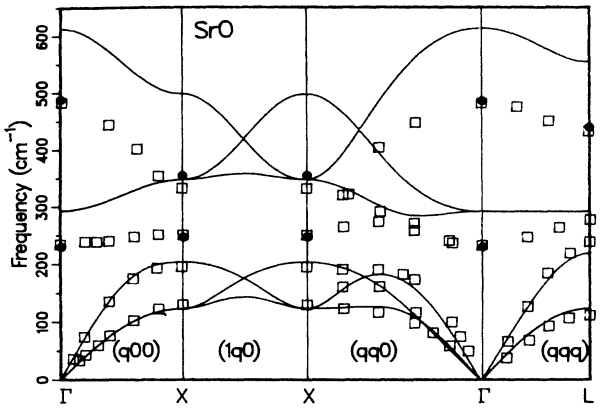

FIG. 3. Phonon dispersion relations for SrO.

The PIB model gives excellent agreement with experiment for the acoustic modes, except possibly in BaO. The LO branch is consistently too high due to the neglect of dipolar charge relaxation. The calculated dispersion of the LO branch, however, agrees well with experiment, except in BaO. However, second-order Raman measurements[23(b)] are consistent with the calculated dispersion which suggests that some of the neutron scattering data for BaO may be in error. Agreement for the TO branch is excellent in MgO, and becomes poorer for the oxides of the larger cations. However, note that the frequency scale for the figures is expanded for the heavier oxides, so that although the percentage error worsens considerably, the absolute error in frequency does not.

The worsening relative error for the oxides of the heavier cations is probably due to the greater polarizability of their atoms. Not only does the cation become more polarizable as the number of electrons increases, but the oxygen is also more polarizable since it is larger due to the expanded structure. Thus neglect of nonspherical polarization is a better approximation for the upper rows of the periodic table than for crystals with larger atoms. At high pressures, properties may be predicted more accu-

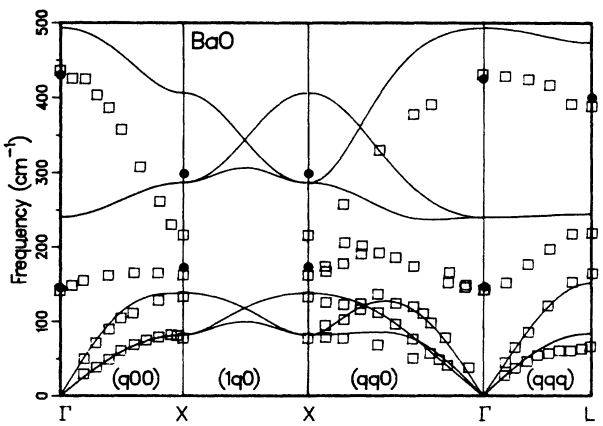

FIG. 4. Phonon dispersion relations for BaO.

rately due to the smaller atoms, which would be dynamically less polarizable, but nonspherical deformation may become increasingly important at extreme pressures.

B. LO-TO splitting

Long-range forces split the frequencies of longitudinal and transverse vibrations for any finite wave vector. If only short-range forces were present, the frequencies would be degenerate in the neighborhood of the zone center since the displacement patterns become identical at $q=0$. Rigid-ion models predict too large an LO-TO splitting. Spherical breathing, however, softens the LO vibrations leading to an LO-TO splitting closer to experiment.[4] In Ref. 4 the self-energy contribution to changes in the LO-TO splitting was considered. There is, however, an overlap contribution as well, which is opposite in sign to that of the self-energy. The overlap contribution arises from sums of the first derivatives of the overlap energy with potentials (A7)—(A12). Table I shows the calculated and observed LO-TO splitting expressed in terms of an effective charge, Y, defined for the $B1$ structure by

$$\omega_{\mathrm{LO}}^2-\omega_{\mathrm{TO}}^2=\frac{4\pi e^2Y^2}{\mu v}\ , \tag{2}$$

where μ is the reduced mass and v is the primitive-cell volume. The results for PIB remain better than $Y=2$ for a rigid-ion model but the LO frequencies are still too high. Agreement is better for the heavier oxides probably because of the greater importance of higher-order polarizabilities, which leads to compensating errors for the LO-TO splitting as well as a lack of agreement with the observed trend from MgO to BaO. The PIB model gives a zeroth-order effect on the LO-TO splitting, but nonspherical charge relaxation is required to obtain better agreement.

The effective charge products for PIB are given in (A12) and (A41); the effective charges in PIB do not sum to zero since the anion is more responsive to changes in the Watson-sphere radius than the cation. In more complex crystals, this leads to irregular frequencies at the zone center, including, for example, splitting of nonpolar Raman modes. The magnitude of the splitting depends significantly on the form used for the kinetic energy part of the self-energy; The Thomas-Fermi form gives large anomalous splittings, whereas the Kohn-Sham kinetic energy gives small splittings. We are investigating whether or not these additional splittings are genuine, or possibly result from a deficiency in the PIB model. Since this is not an issue for $B1$-structured crystals, it will not be discussed further here.

TABLE I. Calculated and experimental effective charges for LO-TO splitting.

	a (Å)	Y_{expt}	Y_{PIB}
MgO	4.30	1.15	1.67
CaO	4.82	1.26	1.62
SrO	5.13	1.40	1.64
BaO	5.51	1.43	1.50

C. Comparison with other models

Nonempirical models such as PIB contrast favorably with empirical models. Much of the lattice-dynamics literature centers on the shell model, which is a mechanical model that describes atoms in crystals as "shells" and "cores" connected by springs. The forces between the various shells and cores are represented by different spring constants, as well as by long-range Coulomb forces resulting from the charges on the shells and cores. The zero Fourier component, or long-range part, of the force-constant matrix is explicitly separated as a macroscopic electric field. In the shell models, the number of parameters proliferates rapidly. These parameters are generally contained by empirically fitting observed crystal properties, sometimes including the dispersion relations which are to be "modeled." Even when the properties are well fit by a set of parameters, the parameters may not represent the forces to which they refer in the model. It has been found, for example, that potentials that describe the defect properties of rutile do not work well for vibrational properties.[24]

In contrast to the empirical approach, more fundamental methods obtain potentials without fitting any experimental data. Elaborate methods have been used to calculate phonon frequencies of, for example, GaAs (Ref. 25) and NaCl (Ref. 26). Such calculations are orders of magnitude more expensive than the simple model presented here. Because of the time and expense involved in such calculations, elaborate methods are restricted to simple structures and frequencies can be obtained only along high-symmetry directions. Results at many wave vectors are required in order to obtain thermal properties such as the equation of state or heat capacity.

Phonon frequencies can be obtained experimentally by optical spectroscopy or inelastic neutron scattering. In order to derive thermodynamic properties from these data, however, it is necessary to interpolate and extrapolate from the measured data, since optical spectroscopy generally measures only some zone-center frequencies and inelastic neutron scattering is generally performed only for symmetry directions. Although neutron scattering data is invaluable in elucidating the vibrational properties of solids, it is very expensive and time consuming, and can be applied only in a limited pressure-temperature environment. Large single crystals are required as well, so that it would be impossible to measure phonon frequencies in quenched high-pressure phases by neutron scattering, for example.

V. CONCLUSIONS

Potential induced breathing is a simple approximation to charge relaxation effects on the vibrational properties of ionic crystals; it greatly improves agreement with experiment for the alkaline-earth oxides over rigid-ion models. The calculated acoustic and elastic properties are quite accurate. The longitudinal-optical branch frequencies are too high due to the neglect of dipolar charge re-

laxation, but are better than rigid-ion frequencies. The transverse-optical frequencies are quite good for MgO and CaO, but become too high for the heavier oxides, since higher-order charge relaxation becomes more important for oxides of the larger cations.

PIB is a model with no adjustable parameters that can provide predictions of properties under conditions that are not experimentally accessible. It can also be used to better understand the implications of experimental observations. Discrepancies between calculated and observed properties can point out important contributions not included in the PIB model.

Possible improvements to the PIB model which would make it more realistic include nonspherical charge relaxation, consideration of local potential differences rather than absolute potentials, use of a better kinetic energy functional, and/or local corrections to the static potentials. Such improvements would probably lead to better predictions but could destroy much of the simplicity of the model. Improvements that retain the computational simplicity of the model are being investigated.

ACKNOWLEDGMENTS

We would like to acknowledge helpful discussions with R. M. Martin, J. R. Hardy, R. J. Hemley, S. R. Chubb, W. E. Pickett, H. Krakauer, J. L. Feldman, and K. L. Cohen. This research was partially supported by the Office of Naval Research under Contract No. N000147WX24121 (R.E.C.) acknowledges support from the National Research Council.

APPENDIX A: DERIVATION OF THE DYNAMICAL MATRIX ELEMENTS

A. The short-range potential

In the PIB model, the short-range potential is

$$U^{\mathrm{SR}}=\tfrac{1}{2}\sum_{\substack{l,k\\ l',k'}}{}'\phi(^{l\ l'}_{k\ k'}) , \tag{A1}$$

where l and l' label primitive cells and k and k' label atomic sites in the primitive cell. The short-range potentials ϕ are functions of the Madelung potentials at $(^{l}_{k})$ and $(^{l'}_{k'})$ as well as the distance $r(^{l\ l'}_{k\ k'})$. Let $r(^{l}_{k})=x(^{l}_{k})+u(^{l}_{k})$, where r is the displaced position of atom $(^{l}_{k})$, x is the equilibrium position, and u is the displacement. The chain rule is used to find the derivatives of U^{SR} with respect to arbitrary displacements. The first derivative of U^{SR} is

$$U^{\mathrm{SR}}_{\alpha}\equiv\left[\frac{\partial U^{\mathrm{SR}}}{\partial r_\alpha(^{m}_{j})}\right]=\tfrac{1}{2}\sum_{\substack{l,k\\ l',k'}}{}'\left[\frac{\partial\phi}{\partial r_\alpha(^{m}_{j})}\right]_{P}^{\mathrm{const}}+\sum_{\substack{l,k\\ l',k'}}{}'\left[\frac{\partial\phi}{\partial P(^{l}_{k})}\right]\left[\frac{\partial P(^{l}_{k})}{\partial r_\alpha(^{m}_{j})}\right] . \tag{A2}$$

The Madelung potential at $(^{l}_{k})$ is given by

$$P(^{l}_{k})=\sum_{l'',k''}{}'\frac{z_{k''}}{r(^{l\ l''}_{k\ k''})} , \tag{A3}$$

and the first derivatives of the site potential are

$$\left[\frac{\partial P(^{l}_{k})}{\partial r_\alpha(^{m}_{j})}\right]=\begin{cases} z_j\dfrac{x_\alpha}{x^3}(^{lm}_{kj}), & (^{l}_{k})\neq(^{m}_{j}) \\ -\displaystyle\sum_{l'',k''}{}' z_{k''}\frac{x_\alpha(^{m\ l''}_{j\ k''})}{x^3}=-E_\alpha(^{m}_{j}), & (^{l}_{k})=(^{m}_{j}) , \end{cases} \tag{A4}$$

where $\mathbf{E}(^{m}_{j})$ is the electric field at $(^{m}_{j})$, $x_\alpha(^{l\ m}_{k\ j})$ is the α component of the vector between $(^{l}_{k})$ and $(^{m}_{j})$, and x is the length of the vector. The atomic and cell indices for the latter are the same as for x_α, and are suppressed. All derivatives are evaluated at the equilibrium positions. Translational invariance is assumed throughout for all potentials and derivatives.

The second derivative of the short-range energy is given by

$$U^{\mathrm{SR}}_{\alpha\beta}\equiv\left[\frac{\partial^2 U^{\mathrm{SR}}}{\partial r_\alpha(^{m}_{j})\partial r_\beta(^{0}_{j'})}\right]=U^{\mathrm{RI}}_{\alpha\beta}+U^{Pr_\alpha}_{\alpha\beta}+U^{Pr_\beta}_{\alpha\beta}+U^{P^2}_{\alpha\beta}+U^{PP}_{\alpha\beta}+U^{P}_{\alpha\beta} , \tag{A5}$$

where

$$\begin{aligned} U^{\mathrm{RI}}_{\alpha\beta}&\equiv\tfrac{1}{2}\sum_{\substack{l,k\\ l',k'}}{}'\left[\frac{\partial^2\phi(^{l\ l'}_{k\ k'})}{\partial r_\alpha(^{m}_{j})\partial r_\beta(^{0}_{j'})}\right]_{P}^{\mathrm{const}} , \\ U^{Pr_\alpha}_{\alpha\beta}&\equiv\sum_{\substack{l,k\\ l',k'}}{}'\left[\frac{\partial^2\phi(^{l\ l'}_{k\ k'})}{\partial r_\alpha(^{m}_{j})\partial P(^{l}_{k})}\right]\left[\frac{\partial P(^{l}_{k})}{\partial r_\beta(^{0}_{j'})}\right] , \\ U^{Pr_\beta}_{\alpha\beta}&\equiv\sum_{\substack{l,k\\ l',k'}}{}'\left[\frac{\partial^2\phi(^{l\ l'}_{k\ k'})}{\partial r_\beta(^{0}_{j'})\partial P(^{l}_{k})}\right]\left[\frac{\partial P(^{l}_{k})}{\partial r_\alpha(^{m}_{j})}\right] , \\ U^{P^2}_{\alpha\beta}&\equiv\sum_{\substack{l,k\\ l',k'}}{}'\left[\frac{\partial^2\phi(^{l\ l'}_{k\ k'})}{\partial P(^{l}_{k})^2}\right]\left[\frac{\partial P(^{l}_{k})}{\partial r_\alpha(^{m}_{j})}\right]\left[\frac{\partial P(^{l}_{k})}{\partial r_\beta(^{0}_{j'})}\right] , \\ U^{PP}_{\alpha\beta}&\equiv\sum_{\substack{l,k\\ l',k'}}{}'\left[\frac{\partial^2\phi(^{l\ l'}_{k\ k'})}{\partial P(^{l}_{k})\partial P(^{l'}_{k'})}\right]\left[\frac{\partial P(^{l}_{k})}{\partial r_\alpha(^{m}_{j})}\right]\left[\frac{\partial P(^{l'}_{k'})}{\partial r_\beta(^{0}_{j'})}\right] , \end{aligned} \tag{A6}$$

and

$$U^{P}_{\alpha\beta}\equiv\sum_{\substack{l,k\\ l',k'}}{}'\left[\frac{\partial\phi(^{l\ l'}_{k\ k'})}{\partial P(^{l}_{k})}\right]\left[\frac{\partial^2 P(^{l}_{k})}{\partial r_\alpha(^{m}_{j})\partial r_\beta(^{0}_{j'})}\right] .$$

The first term in (A2) and $U^{\mathrm{RI}}_{\alpha\beta}$ in (A6) are rigid-ion contributions. The other terms are PIB contributions and are many-body in nature. We now turn our attention to these.

$U^{P}_{\alpha\beta}$ can be simplified from a double sum to a single sum

$$U^{P}_{\alpha\beta}=\sum_{l,k}c_k\left[\frac{\partial^2 P(^{l}_{k})}{\partial r_\alpha(^{m}_{j})\partial r_\beta(^{0}_{j'})}\right] , \tag{A7}$$

where

$$c_k \equiv \sum_{l',k}{}' \left[\frac{\partial \phi(^{0\ l'}_{k\ k'})}{\partial P(^{0}_{k})} \right] . \tag{A8}$$

$U^P_{\alpha\beta}$ is identical in form to the second derivative of the Madelung energy given by

$$U^{c,\mathrm{RI}}_{\alpha\beta} = \tfrac{1}{2} \sum_{l,k} z_k \left[\frac{\partial^2 P(^{l}_{k})}{\partial r_\alpha(^{m}_{j}) \partial r_\beta(^{0}_{j'})} \right] . \tag{A9}$$

An effective charge product is defined as

$$f_{kk'} \equiv c_k z_{k'} + c_{k'} z_k \tag{A10}$$

so that we write

$$U^P_{\alpha\beta} = \tfrac{1}{2} \sum_{\substack{l,k \\ l',k'}}{}' f_{kk'} \left[\frac{\partial^2}{\partial r_\alpha(^{m}_{j}) \partial r_\beta(^{0}_{j'})} \left[\frac{1}{r(^{l\ l'}_{k\ k'})} \right] \right] , \tag{A11}$$

and Kellerman's method[13] is used to find the contributions to the dynamical matrix. The effective charge factor (A10) leads to a replacement in the Kellerman formula of $z_k z_{k'}$ by $z_{kk'}$ where

$$z_{kk'} \equiv \begin{cases} z_k z_{k'} + c_k z_{k'} + c_{k'} z_k, & k \neq k' \\ z_k^2 + 2 c_k z_k - z_k \sum_{k'} c_{k'}, & k = k' \end{cases} \tag{A12}$$

and the $k = k'$ value for z_{kk} follows from translational invariance.

Next $U^{Pr_\alpha}_{\alpha\beta}$ and $U^{Pr_\beta}_{\alpha\beta}$ are considered. Firstly, the double sum $U^{Pr_\alpha}_{\alpha\beta}$ is split into two single sums

$$\begin{aligned} U^{Pr_\alpha}_{\alpha\beta} = & \sum_{l,k}{}' \left[\frac{\partial^2 \phi(^{l\ m}_{k\ j})}{\partial r_\alpha(^{m}_{j}) \partial P(^{l}_{k})} \right] \left[\frac{\partial P(^{l}_{k})}{\partial r_\beta(^{0}_{j'})} \right] \\ & + \sum_{l,k}{}' \left[\frac{\partial^2 \phi(^{m\ l}_{j\ k})}{\partial r_\alpha(^{m}_{j}) \partial P(^{m}_{j})} \right] \left[\frac{\partial P(^{m}_{j})}{\partial r_\beta(^{0}_{j'})} \right] . \end{aligned} \tag{A13}$$

The other terms in $U^{Pr_\alpha}_{\alpha\beta}$ are zero. Using (A4), the first sum in (A13) is

$$\sum_{l,k}{}' \left[\frac{\partial^2 \phi(^{l\ m}_{k\ j})}{\partial r_\alpha(^{m}_{j}) \partial P(^{l}_{k})} \right] \left[\frac{\partial P(^{l}_{k})}{\partial r_\beta(^{0}_{j'})} \right] = \sum_{l,k}{}' \left[\frac{\partial^2 \phi(^{l\ m}_{k\ j})}{\partial r_\alpha(^{m}_{j}) \partial P(^{l}_{k})} \right] \left[z_{j'} \frac{x_\beta(^{l\ 0}_{k\ j'})}{x^3} [1 - \delta(^{l\ 0}_{k\ j'})] - E_\beta(^{0}_{j'}) \delta(^{l\ 0}_{k\ j'}) \right] , \tag{A14}$$

where $\delta(^{l\ 0}_{k\ j'})$ is one if $(^{l}_{k}) = (^{0}_{j'})$, and zero otherwise.

The dynamical matrix is given by[15]

$$D_{\alpha\beta}(jj',\mathbf{q}) = \frac{e^{-i\mathbf{q}\cdot\mathbf{x}(jj')}}{(M_j M_{j'})^{1/2}} \sum_m e^{-i\mathbf{q}\cdot\mathbf{x}(m)} U_{\alpha\beta} . \tag{A15}$$

The prefactor will be omitted below until each equation is summarized. The contribution to the dynamical matrix from (A14) is

$$\sum_k \left[\sum_m{}' e^{-i\mathbf{q}\cdot\mathbf{x}(m)} \left[\frac{\partial^2 \phi(^{0\ m}_{k\ j})}{\partial r_\alpha(^{m}_{j}) \partial P(^{0}_{k})} \right] \right] \sum_l e^{i\mathbf{q}\cdot\mathbf{x}(l)} \left[z_{j'} \frac{x_\beta(^{0\ l}_{k\ j'})}{x^3} [1 - \delta(^{0\ l}_{k\ j'})] - E_\beta(^{0}_{j'}) \delta(^{0\ l}_{k\ j'}) \right] , \tag{A16}$$

where translational invariance has been used to separate the m and l sums. The m sum converges rapidly for the short-range potential. The l sum, however, is only slowly convergent. Sums such as

$$\Theta_\alpha(kj,\mathbf{q}) = \sum_m{}' e^{-i\mathbf{q}\cdot\mathbf{x}(m)} \frac{x_\alpha(^{0\ m}_{k\ j})}{x^3} \tag{A17}$$

occur frequently here. A rapidly convergent Ewald-type transformation for this sum is discussed in Appendix B. Using this symbolism the dynamical matrix contribution from the first sum in (A13) is given by

$$D^{Pr_{\alpha'}1}_{\alpha\beta} = \frac{e^{-i\mathbf{q}\cdot\mathbf{x}(jj')}}{(M_j M_{j'})^{1/2}} \sum_k p^*_\alpha(k_j) [z_{j'} \Theta^*_\beta(kj') - E_\beta(j') \delta_{kj'}] , \tag{A18}$$

where

$$p_\alpha(kj) \equiv - \sum_m{}' e^{-i\mathbf{q}\cdot\mathbf{x}(m)} \left[\frac{\partial^2 \phi(^{m\ 0}_{k\ j})}{\partial x \partial P(k)} \right] \frac{x_\alpha(^{m\ 0}_{k\ j})}{x} . \tag{A19}$$

Next, consider the second sum in (A13):

$$\begin{aligned} \sum_m \sum_{l,k}{}' e^{-i\mathbf{q}\cdot\mathbf{x}(m)} \left[\frac{\partial^2 \phi(^{m\ l}_{j\ k})}{\partial r_\alpha(^{m}_{j}) \partial P(^{m}_{j})} \right] \left[\frac{\partial P(^{m}_{j})}{\partial r_\beta(^{0}_{j'})} \right] = & \sum_k \sum_m e^{-i\mathbf{q}\cdot\mathbf{x}(m)} \left[z_{j'} \frac{x_\beta(^{m\ 0}_{j\ j'})}{x^3} [1 - \delta(^{m\ 0}_{j\ j'})] - E_\beta(^{0}_{j}) \delta(^{m\ 0}_{j\ j'}) \right] \\ & \times \sum_l{}' \left[\frac{\partial^2 \phi(^{0\ l}_{j\ k})}{\partial r_\alpha(^{0}_{j}) \partial P(^{0}_{j})} \right] . \end{aligned} \tag{A20}$$

The dynamical matrix contribution is

$$D_{\alpha\beta}^{Pr_{\alpha'},2}=\frac{e^{-i\mathbf{q}\cdot\mathbf{x}(jj')}}{(M_jM_{j'})^{1/2}}d_{j\alpha}[z_{j'}\Theta_\beta^*(jj')-E_\beta(j')\delta_{jj'}]\ , \tag{A21}$$

where

$$d_{j\alpha}\equiv\sum_{l,k}{}'\left[\frac{\partial^2\phi(^{0\ l}_{j\ k})}{\partial x\partial P(j)}\right]\frac{x_\alpha(^{0\ l}_{j\ k})}{x}\ . \tag{A22}$$

We continue with the sum

$$U_{\alpha\beta}^{Pr_\beta}=\sum_{l,k}{}'\left[\frac{\partial^2\phi(^{l\ 0}_{k\ j'})}{\partial r_\beta(^0_{j'})\partial P(^l_k)}\right]\left[\frac{\partial P(^l_k)}{\partial r_\alpha(^m_j)}\right]+\sum_{l,k}{}'\left[\frac{\partial^2\phi(^{0\ l}_{j'\ k})}{\partial r_\beta(^0_{j'})\partial P(^0_{j'})}\right]\left[\frac{\partial P(^0_{j'})}{\partial r_\alpha(^m_j)}\right]\ . \tag{A23}$$

The first sum in (A23) contributes

$$\sum_m\sum_{l,k}{}'e^{-i\mathbf{q}\cdot\mathbf{x}(m)}\left[\frac{\partial^2\phi(^{l\ 0}_{k\ j'})}{\partial r_\beta(^0_{j'})\partial P(^l_k)}\right]\left[z_j\frac{x_\alpha(^{l\ m}_{k\ j})}{x^3}[1-\delta(^{l\ m}_{k\ j})]-E_\alpha(j)\delta(^{l\ m}_{k\ j})\right]\ . \tag{A24}$$

Let $l'=m-1$ so (A24) becomes

$$\sum_k\left[\sum_l{}'e^{-i\mathbf{q}\cdot\mathbf{x}(l)}\left[\frac{\partial^2\phi(^{l\ 0}_{k\ j'})}{\partial r_\beta(^0_{j'})\partial P(^l_k)}\right]\right]\left[z_j\Theta_\alpha(k_j)-E_\alpha(j)\delta_{kj}\right]\ , \tag{A25}$$

and we get

$$D_{\alpha\beta}^{Pr_\beta,1}=\frac{e^{-i\mathbf{q}\cdot\mathbf{x}(jj')}}{(M_jM_{j'})^{1/2}}\sum_k p_\beta(kj')[z_j\Theta_\alpha(k_j)-E_\alpha(j)\delta_{kj}]\ , \tag{A26}$$

where $\mathbf{p}$ is defined in (A19).

The last sum containing one first derivative of electrostatic potential with displacement is given by the second term in (A23). The dynamical matrix contribution is

$$\sum_m e^{-i\mathbf{q}\cdot\mathbf{x}(m)}\sum_{l,k}{}'\left[\frac{\partial^2\phi(^{0\ l}_{j'\ k})}{\partial r_\beta(^0_{j'})\partial P(^0_{j'})}\right]\left[z_j\frac{x_\alpha(^{0\ m}_{j'\ j})}{x^3}-E_\alpha(j)\delta(^{0\ m}_{j'\ j})\right]\ , \tag{A27}$$

which is similar to (A20) and gives

$$D_{\alpha\beta}^{Pr_\beta,2}=\frac{e^{-i\mathbf{q}\cdot\mathbf{x}(jj')}}{(M_jM_{j'})^{1/2}}d_{j'\beta}[z_j\Theta_\alpha(j'j)-E_\alpha(j)\delta_{j'j}]\ , \tag{A28}$$

where $\mathbf{d}$ is defined in (A22).

Next, consider $U_{\alpha\beta}^{P^2}$. The dynamical matrix contribution is

$$\sum_m\sum_{l,k}{}'t_k\left[z_j\frac{x_\alpha(^{l\ m}_{k\ j})}{x^3}[1-\delta(^{l\ m}_{k\ j})]-E_\alpha(^m_j)\delta(^{l\ m}_{k\ j})\right]\left[z_{j'}\frac{x_\beta(^{l\ 0}_{k\ j'})}{x^3}[1-\delta(^{l\ 0}_{k\ j'})]-E_\beta(^0_{j'})\delta(^{l\ 0}_{k\ j'})\right]e^{-i\mathbf{q}\cdot\mathbf{x}(m)}\ , \tag{A29}$$

where

$$t_k\equiv\sum_{l,k'}{}'\left[\frac{\partial^2\phi(^{0\ l'}_{k\ k'})}{\partial P_k^2}\right]\ . \tag{A30}$$

Letting $m'=m-1$, we have

$$\sum_k\sum_l t_k\left[z_{j'}\frac{x_\beta(^{l\ 0}_{k\ j'})}{x^3}[1-\delta(^{l\ 0}_{k\ j'})]-E_\beta(j')\delta(^{l\ 0}_{k\ j'})\right]e^{-i\mathbf{q}\cdot\mathbf{x}(l)}\sum_{m'}\left[z_j\frac{x_\alpha(^{0\ m'}_{k\ j})}{x^3}[1-\delta(^{0\ m'}_{k\ j})]-E_\alpha(^{m'}_j)\delta(^{0\ m'}_{k\ j})\right]e^{-i\mathbf{q}\cdot\mathbf{x}(m')}\ . \tag{A31}$$

The l and m' sums are completely factored in (A31) and we find

$$D_{\alpha\beta}^{P^2}=\frac{e^{-i\mathbf{q}\cdot\mathbf{x}(jj')}}{(M_jM_{j'})^{1/2}}\sum_k t_k[z_j\Theta_\alpha(k_j)-E_\alpha(j)\delta_{kj}][z_{j'}\Theta_\beta^*(kj')-E_\beta(j')\delta_{kj'}]\ , \tag{A32}$$

where t_k is defined in (A30).

The final short-range sum to consider, $U^{PP}_{\alpha\beta}$, contributes

$$\sum_m \sum_{l,k} \sum_{l',k'}{}' \left[\frac{\partial^2 \phi(^{l\ l'}_{k\ k'})}{\partial P(^{l}_{k}) \partial P(^{l'}_{k'})} \right] \left[z_j \frac{x_\alpha(^{l\ m}_{k\ j})}{x^3} [1-\delta(^{l\ m}_{k\ j})] - E_\alpha(^{m}_{j}) \delta(^{l\ m}_{k\ j}) \right] \left[z_{j'} \frac{x_\beta(^{l'\ 0}_{k'\ j'})}{x^3} [1-\delta(^{l'\ 0}_{k'\ j'})] - E_\beta(^{0}_{j'}) \delta(^{l'\ 0}_{k'\ j'}) \right] e^{-i\mathbf{q}\cdot\mathbf{x}(m)} \tag{A33}$$

to the dynamical matrix. Let $m' = m - 1$ and find

$$\sum_{l,k} \sum_{l',k'}{}' \left[\frac{\partial^2 \phi(^{l\ l'}_{k\ k'})}{\partial P(^{l}_{k}) \partial P(^{l'}_{k'})} \right] \left[z_{j'} \frac{x_\beta(^{l'\ 0}_{k'\ j'})}{x^3} [1-\delta(^{l'\ 0}_{k'\ j'})] - E_\beta(^{0}_{j'}) \delta(^{l'\ 0}_{k'\ j'}) \right] e^{-i\mathbf{q}\cdot\mathbf{x}(l)} [z_j \Theta_\alpha(k_j) - E_\alpha(j)\delta_{kj}] \ . \tag{A34}$$

Now, let $l'' = l - l'$ and get

$$\sum_k [z_j \Theta_\alpha(k_j) - E_\alpha(j)\delta_{kj}] \sum_{k'} \left[\sum_{l''} \left[\frac{\partial^2 \phi(^{l''\ 0}_{k\ k'})}{\partial P(^{l''}_{k}) \partial P(^{0}_{k'})} \right] e^{-i\mathbf{q}\cdot\mathbf{x}(l'')} \right] [z_{j'} \Theta^*_\beta(k'j') - E_\beta(j')\delta_{k'j'}] \ , \tag{A35}$$

and finally

$$D^{PP}_{\alpha\beta} = \frac{e^{-i\mathbf{q}\cdot\mathbf{x}(jj')}}{(M_j M_{j'})^{1/2}} \sum_k \sum_{k'} g(kk',\mathbf{q}) [z_j \Theta_\alpha(kj) - E_\alpha(j)\delta_{jk}] [z_{j'} \Theta^*_\beta(k'j') - E_\beta(j')\delta_{k'j'}] \ , \tag{A36}$$

where

$$g(kk',\mathbf{q}) \equiv \sum_l{}' \left[\frac{\partial^2 \phi(^{l\ 0}_{k\ k'})}{\partial P(^{l}_{k}) \partial P(^{0}_{k'})} \right] e^{-i\mathbf{q}\cdot\mathbf{x}(l)} \ . \tag{A37}$$

B. The self-energy

Now we must consider the self-energy contributions to PIB lattice dynamics. The self-energy is given by

$$U^{\mathrm{SE}} = \sum_{l,k} S(^{l}_{k}) \ . \tag{A38}$$

The derivatives with respect to arbitrary displacements are

$$U^{\mathrm{SE}}_\alpha \equiv \left[\frac{\partial U^{\mathrm{SE}}}{\partial r_\alpha(^{m}_{j})} \right] = \sum_{l,k} \left[\frac{\partial S(^{l}_{k})}{\partial P(^{l}_{k})} \right] \left[\frac{\partial P(^{l}_{k})}{\partial r_\alpha(^{m}_{j})} \right] \tag{A39}$$

and

$$\begin{aligned} U^{\mathrm{SE}}_{\alpha\beta} &\equiv \left[\frac{\partial^2 U^{\mathrm{SE}}}{\partial r_\alpha(^{m}_{j}) \partial r_\beta(^{0}_{j'})} \right] \\ &= \sum_{l,k} \left[\frac{\partial S(^{l}_{k})}{\partial P(^{l}_{k})} \right] \left[\frac{\partial^2 P(^{l}_{k})}{\partial r_\alpha(^{m}_{j}) \partial r_\beta(^{0}_{j'})} \right] \\ &\quad + \sum_{l,k} \left[\frac{\partial^2 S(^{l}_{k})}{\partial P(^{l}_{k})^2} \right] \left[\frac{\partial P(^{l}_{k})}{\partial r_\alpha(^{m}_{j})} \right] \left[\frac{\partial P(^{l}_{k})}{\partial r_\beta(^{0}_{j'})} \right] \ . \end{aligned} \tag{A40}$$

The first sum in (A40) is identical in form to (A7) and gives an additional effective charge contribution,

$$c'_k \equiv \sum_{l',k'}{}' \left[\frac{\partial \phi(^{0\ l'}_{k\ k'})}{\partial P(^{0}_{k})} \right] + \left[\frac{\partial S(k)}{\partial P(k)} \right] \ . \tag{A41}$$

The second sum in (A40) leads to a dynamical matrix contribution identical in form to (A32) with

$$t'_k \equiv \sum_{l',k'}{}' \left[\frac{\partial^2 \phi(^{0\ l'}_{k\ k'})}{\partial P^2_k} \right] + \frac{\partial^2 S(k)}{\partial P^2_k} \ . \tag{A42}$$

APPENDIX B: A RAPIDLY CONVERGENT FORM FOR THE Θ SUM

A rapidly convergent form for the lattice sum

$$\Theta_\alpha(kj;\mathbf{q}) \equiv \sum_m{}' e^{-i\mathbf{q}\cdot\mathbf{x}(m)} \frac{x_\alpha(^{0\ m}_{k\ j})}{x^3} \tag{B1}$$

must be found. An Ewald-type method is used to write the sum as rapidly convergent direct-space and reciprocal-space lattice sums. The Θ sum, (B1), is a derivative of a general type of lattice sum discussed by Tosi,[16] and is

$$\Theta_\alpha(kj,\mathbf{q}) = -\sum_m{}' e^{-i\mathbf{q}\cdot\mathbf{x}(m)} \left[\frac{\partial}{\partial x_\alpha(k)} \left[\frac{1}{x(^{0\ m}_{k\ j})} \right] \right] \ . \tag{B2}$$

Using the identity

$$\frac{1}{|r|} = \frac{2}{\sqrt{\pi}} \int_0^\infty e^{-t^2 r^2} dt \ , \tag{B3}$$

we have

$$-\frac{\partial}{\partial x_\alpha(k)} \int_0^\infty \frac{2}{\sqrt{\pi}} \sum_m \exp[-t^2 x^2(^{0\ m}_{k\ j}) - i\mathbf{q}\cdot\mathbf{x}(m)] dt \ . \tag{B4}$$

We split the integral into two parts, an integral from 0 to ϵ, and one from ϵ to ∞, where ϵ is a convergence parameter, and use the theta transformation,[16] given by

$$\begin{aligned} &\frac{2}{\sqrt{\pi}} \sum_m \exp[-t^2 x^2(^{0\ m}_{k\ j}) - i\mathbf{q}\cdot\mathbf{x}(m)] \\ &\quad = \frac{2\pi}{v} \sum_{\mathbf{Q}} \frac{1}{t^3} \exp\left[\frac{-|\mathbf{Q}+\mathbf{q}|^2}{4t^2} - i(\mathbf{Q}+\mathbf{q})\cdot\mathbf{x}(kj) \right] \end{aligned} \tag{B5}$$

where v is the primitive cell volume and $\mathbf{Q}$ is a reciprocal-lattice vector, in the first integral giving

$$-\frac{2\pi}{v}\sum_{Q}\frac{\partial}{\partial x_\alpha(x)}\{\exp[-i(\mathbf{Q}+\mathbf{q})\cdot\mathbf{x}(k_j)]\}\times\int_0^\epsilon\frac{1}{t^3}\exp\left[\frac{-|\mathbf{Q}+\mathbf{q}|^2}{4t^2}\right]dt\ . \quad \text{(B6)}$$

The integral in (B6) is

$$\int_0^\epsilon t^{-3}e^{-at^{-2}}dt=\frac{1}{2a}e^{-a/\epsilon^2}\ , \quad \text{(B7)}$$

so we have

$$-\frac{4\pi}{v}\sum_{Q}\frac{\exp\left[-\frac{|\mathbf{Q}+\mathbf{q}|^2}{4\epsilon^2}\right]}{|\mathbf{Q}+\mathbf{q}|^2}\frac{\partial}{\partial x_\alpha(k)}\{\exp[-i(\mathbf{Q}+\mathbf{q})\cdot\mathbf{x}(kj)]\}=\frac{4\pi}{v}\sum_{Q}\frac{i(Q_\alpha+q_\alpha)}{|\mathbf{Q}+\mathbf{q}|^2}\exp\left[\frac{-|\mathbf{Q}+\mathbf{q}|^2}{4\epsilon^2}-i(\mathbf{Q}+\mathbf{q})\cdot\mathbf{x}(kj)\right] \quad \text{(B8)}$$

for the reciprocal lattice sum.

The second integral is

$$\begin{aligned}-\frac{\partial}{\partial x_\alpha(k)}\int_\epsilon^\infty\frac{2}{\sqrt{\pi}}\sum_m\exp[-t^2x^2(^0_{kj}{}^m_{})-i\mathbf{q}\cdot\mathbf{x}(m)]dt&=-\sum_m e^{-i\mathbf{q}\cdot\mathbf{x}(m)}\frac{\partial}{\partial x_\alpha(k)}\left[\frac{2}{\sqrt{\pi}}\int_\epsilon^\infty e^{-t^2x^2(^0_{kj}{}^m_{})}dt\right]\\&=-\sum_m e^{-i\mathbf{q}\cdot\mathbf{x}(m)}\frac{\partial}{\partial x_\alpha(k)}\left[\frac{1}{x(^0_{kj}{}^m_{})}\operatorname{erfc}[\epsilon x(^0_{kj}{}^m_{})]\right]\\&=\sum_m e^{-i\mathbf{q}\cdot\mathbf{x}(m)}\left[\frac{2\epsilon}{\sqrt{\pi}}\frac{x_\alpha(^0_{kj}{}^m_{})}{x^2}e^{-\epsilon^2x^2(^0_{kj}{}^m_{})}\right.\\&\quad\left.+\frac{x_\alpha(^0_{kj}{}^m_{})}{x^3}\operatorname{erfc}[\epsilon x(^0_{kj}{}^m_{})]\right]\ . \quad \text{(B9)}\end{aligned}$$

The behavior of (B8) and (B9) when $k=j$ must be considered, since when this occurs, the $m=0$ term is omitted in the Θ sum. One finds that the sum (B8) is unaffected, and one need only omit the $m=0$ term in (B9) if $k=j$. Finally we have

$$\begin{aligned}\Theta_\alpha(kj;\mathbf{q})=&\frac{4\pi}{v}\sum_{Q}\frac{i(Q_\alpha+q_\alpha)}{|\mathbf{Q}+\mathbf{q}|^2}\exp\left[-i(\mathbf{Q}+\mathbf{q})\cdot\mathbf{x}(kj)-\frac{|\mathbf{Q}+\mathbf{q}|^2}{4\epsilon^2}\right]\\&+\sum_m{}'e^{-i\mathbf{q}\cdot\mathbf{x}(m)}\left[\frac{2\epsilon}{\sqrt{\pi}}\frac{x_\alpha(^0_{kj}{}^m_{})}{x^2}e^{-\epsilon^2x^2(^0_{kj}{}^m_{})}+\frac{x_\alpha(^0_{kj}{}^m_{})}{x^3}\operatorname{erfc}[\epsilon x(^0_{kj}{}^m_{})]\right]\ . \quad \text{(B10)}\end{aligned}$$

APPENDIX C: THE POLARIZATION SHIFT

A longitudinal polarization wave sets up a potential wave that shifts the local electrostatic zero for the PIB effect. The induced potential is

$$\nabla^2\Phi^s=4\pi\nabla\cdot\mathscr{P}\ , \quad \text{(C1)}$$

where $\mathscr{P}$ is the polarization. To define a local zero, we must take a macroscopic average, relative to the atomic size. A macroscopic average of a microscopic variable can be written as[27]

$$\langle F\rangle=\int d^3x' f(\mathbf{x}')F(\mathbf{x}-\mathbf{x}')\ . \quad \text{(C2)}$$

A spherical average is used for simplicity, and the weighting function f is taken as a Gaussian, since a Gaussian distribution has useful properties,

$$f(\mathbf{x})=(\pi R^2)^{-3/2}e^{-x^2/R^2}\ , \quad \text{(C3)}$$

where R is the length scale. Now the macroscopic polarization is given by

$$\mathscr{P}(\mathbf{x})=\left\langle\sum_n \mathscr{p}_n\delta(\mathbf{x}-\mathbf{x}_n)\right\rangle\ . \quad \text{(C4)}$$

In a complex crystal, we have

$$\mathbf{x}_n=\mathbf{x}(^l_k)\ , \quad \text{(C5)}$$

and

$$\mathscr{p}(^l_{kj}{}^0_{})=\exp[-i\mathbf{q}\cdot\mathbf{x}(^l_{kj}{}^0_{})]\mathbf{A}(kj,\mathbf{q}) \quad \text{(C6)}$$

is the microscopic polarization at (^l_k) relative to sublattice j. $\mathbf{A}(kj,\mathbf{q})$ is the polarization amplitude. The macroscopic polarization from sublattice k on sublattice j is

$$\mathscr{P}(kj)=\mathbf{A}(kj,\mathbf{q})\int d^3x'(\pi R^2)^{-3/2}e^{-(x')^2/R^2}\sum_l \exp[-i\mathbf{q}\cdot\mathbf{x}(^{l\ 0}_{k\ j})]\delta(\mathbf{x}(^{l\ 0}_{k\ j})-\mathbf{x}')$$

$$=e^{-i\mathbf{q}\cdot\mathbf{x}(kj)}\mathbf{A}(kj,\mathbf{q})(\pi R^2)^{-3/2}\sum_l e^{-i\mathbf{q}\cdot\mathbf{x}(l)}e^{-|\mathbf{x}-\mathbf{x}(l)|^2/R^2}\ . \tag{C7}$$

We use the theta transformation (B5) and get

$$\mathscr{P}(kj)=\mathbf{A}(kj,\mathbf{q})\frac{1}{v}\sum_Q \exp\left[\frac{-|\mathbf{Q}+\mathbf{q}|^2R^2}{4}-i(\mathbf{Q}+\mathbf{q})\cdot\mathbf{x}(kj)\right]\ . \tag{C8}$$

Finally, we use (C1) and take the derivative with respect to the α Cartesian component of the polarization amplitude and get

$$\left[\frac{\partial\Phi^s}{\partial A_\alpha}\right]=\frac{4\pi}{v}\sum_Q \frac{i(Q_\alpha+q_\alpha)}{|\mathbf{Q}+\mathbf{q}|^2}\exp\left[\frac{-|\mathbf{Q}+\mathbf{q}|^2R^2}{4}-i(\mathbf{Q}+\mathbf{q})\cdot\mathbf{x}(kj)\right]\ . \tag{C9}$$

The integration constant is zero, so that (C9) goes to zero as the volume is expanded to infinity as in the definition of the Ewald potential.

Equation (C9) is subtracted from the theta sum (B10) to give physically meaningful results within the PIB model. Equation (C9) is equal to the reciprocal-space sum in the Θ sum (B10) for an ϵ equal to $1/R$. Thus the subtraction of (C9) from (B10) is equivalent to evaluating only the direct-space sum in (B10) for an $\epsilon=1/R$. There is no correction to the PIB Kellerman-type coefficients, since $(\partial^2\Phi^s/\partial A_\alpha\partial A_\beta)=0$.

R is chosen so that a sphere of radius R has the volume of the primitive unit cell. This choice for R minimizes the effect of the local shift of the longitudinal mode frequencies, and gives the same elastic constants as are found by static deformations using PIB potentials. R does not effect the frequencies at the zone center or zone boundary. Varying R by 20—50% has negligible effect on the dispersion curves.

[1]R. G. Gordon and Y. S. Kim, J. Chem. Phys. **56**, 3122 (1972); M. Waldman and R. G. Gordon, *ibid.* **71**, 1325 (1979).

[2](a) A. J. Cohen and R. G. Gordon, Phys. Rev. B **12**, 3228 (1975); (b) C. Muhlhausen and R. G. Gordon, *ibid.* **23**, 900 (1981); (c) **24**, 2147 (1981); (d) C. W. Burnham, Rev. Min. **14**, 347 (1985); (e) R. J. Hemley and R. G. Gordon, J. Geophys. Res. B **90**, 7803 (1985); (f) R. J. Hemley, M. D. Jackson, and R. G. Gordon, Geophys. Res. Lett. **12**, 247 (1985); (g) R. E. Cohen and C. W. Burnham, Am. Mineral. **70**, 559 (1985).

[3](a) R. E. Watson, Phys. Rev. **111**, 1108 (1958); (b) E. Paschalis and A. Weiss, Theoret. Chim. Acta **13**, 381 (1969); (c) A. J. Cohen and R. G. Gordon, Phys. Rev. B **14**, 4593 (1976).

[4]L. L. Boyer *et al.*, Phys. Rev. Lett. **54**, 1940 (1985); **57**, 2331 (1986).

[5](a) M. J. Mehl and L. L. Boyer, Bull. Am. Phys. Soc. **29**, 466 (1984); (b) M. J. Mehl, R. J. Hemley, and L. L. Boyer, Phys. Rev. B **33**, 8685 (1986); (c) R. E. Cohen, Geophys. Res. Lett. **14**, 37 (1987); (d) R. E. Cohen, L. L. Boyer, and M. J. Meyl, Phys. Chem. Minerals (to be published).

[6]C. R. A. Catlow, M. Dixon, and W. C. Mackrodt, in *Computer Simulation of Solids*, edited by C. R. A. Catlow and W. C. Mackrodt (Springer-Verlag, New York, 1982).

[7]B. J. Dick and A. W. Overhauser, Phys. Rev. **112**, 90 (1958); A. D. B. Woods, W. Cochran, and B. N. Brockhouse, *ibid.* **119**, 980 (1960).

[8]H. Bilz and W. Kress, *Phonon Dispersion Relations in Insulators*, Vol. 10 of *Springer Series in Solid State Sciencies*, edited by M. Cardona and P. Fulde (Springer-Verlag, Berlin, 1979).

[9](a) L. L. Boyer, Phys. Rev. Lett. **42**, 584 (1979); (b) Ferroelectrics **35**, 83 (1981); (c) J. Phys. C **17**, 1825 (1984); (d) J.W. Flocken, R. A. Guenther, J. R. Hardy, and L. L. Boyer, Phys. Rev. B **31**, 7252 (1985).

[10]L. L. Boyer, Phys. Rev. Lett. **45**, 1858 (1980); Phase Trans. **5**, 1 (1985); M. J. Mehl and L. L. Boyer, Phys. Rev. Lett. **54**, 1404 (1985).

[11]P. Hohenberg and W. Kohn, Phys. Rev. B **136**, 864 (1964); W. E. Pickett, Comments Solid State Phys. **12**, 1 (1985).

[12]B. M. Klein, W. E. Pickett, L. L. Boyer, and R. Zeller, Phys. Rev. B (to be published).

[13]E. W. Kellerman, Philos. Trans. R. Soc. London, Ser. A **238**, 513 (1940).

[14]M. Born and K. Huang, *Dynamical Theory of Crystal Lattices* (Oxford University Press, London, 1954).

[15]L. L. Boyer, Phys. Rev. B **9**, 2684 (1974).

[16]M. P. Tosi, Solid State Phys. **16**, 1 (1964).

[17]W. Kohn and L. J. Sham, Phys. Rev. **140**, A1133 (1965).

[18]D. A. Liberman, D. T. Cromer, and J. J. Walker, Comput. Phys. Commun. **2**, 107 (1971).

[19]L. Hedin and B. I. Lundqvist, J. Phys. C **4**, 2064 (1971).

[20]J. P. Perdew and A. Zunger, Phys. Rev. B **23**, 5048 (1981).

[21]L. H. Thomas, Proc. Cambridge Philos. Soc. **23**, 542 (1926); E. Fermi, Z. Phys. **48**, 73 (1928).

[22](a) M. J. L. Sangster, G. Peckham, and D. H. Saunderson, J. Phys. C **3**, 1026 (1970); (b) D. H. Saunderson and G. Peckham, *ibid.* **4**, 2009 (1971); (c) K. H. Rieder, R. Migoni, and B. Renker, Phys. Rev. B **12**, 3374 (1975); (d) S. A. Chang, C. W. Tompson, E. Gürmen, and L. D. Muhlestein, J. Phys. Chem. Solids **36**, 769 (1975).

[23](a) N. B. Manson, W. von der Ohe, and S. L. Chodos, Phys. Rev. B **3**, 1968 (1971); (b) K. H. Rieder, B. A. Weinstein, Manuel Cardona, and H. Bilz, Phys. Rev. B **8**, 4780 (1973).
[24]M. Mostoller and J. C. Wang, Phys. Rev. B **32**, 6773 (1985).
[25]K. Kunc and R. M. Martin, Phys. Rev. Lett. **48**, 406 (1982).
[26]S. Froyen and M. L. Cohen, Phys. Rev. B **29**, 3770 (1984).
[27]J. D. Jackson, *Classical Electrodynamics* (Wiley, New York, 1975).